Article

Cell Host & Microbe

Autophagy Proteins Promote Repair of Endosomal Membranes Damaged by the *Salmonella* Type Three Secretion System 1

Graphical Abstract

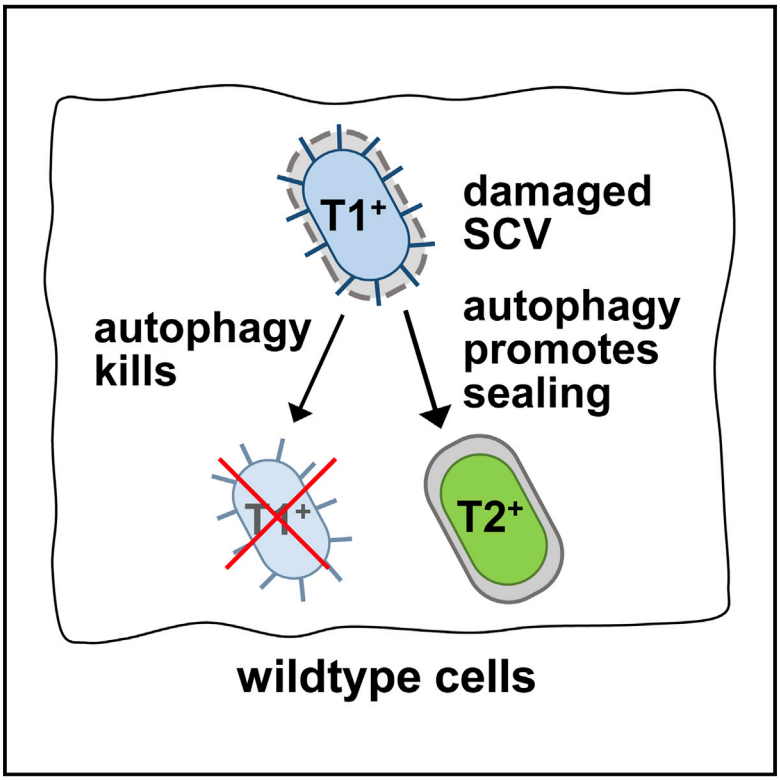

Authors

Saskia Kreibich, Mario Emmenlauer, Jennifer Fredlund, ..., Christoph Dehio, Jost Enninga, Wolf-Dietrich Hardt

Correspondence

hardt@micro.biol.ethz.ch

In Brief

Salmonella Typhimurium employs type three secretion systems (TTSS) that inject effectors into host cells while also likely inflicting membrane damage. Kreibich et al. analyzed the fate of *Salmonella*-containing vacuoles (SCVs) after epithelial cell invasion and find that autophagy promotes repair of TTSS-1-inflicted damage to SCV membranes early during infection.

Highlights

- RNAi screen implicates autophagy in *Salmonella*-containing vacuole (SCV) maintenance
- Autophagy promotes repair of TTSS-1-damaged SCV membranes and TTSS-2 expression
- In parallel, autophagy eliminates cytosolic *Salmonella*
- Autophagy could play a general role in maintaining endosomal membrane integrity

Kreibich et al., 2015, Cell Host & Microbe *18*, 527–537
November 11, 2015
http://dx.doi.org/10.1016/j.chom.2015.10.015

CellPress

Cell Host & Microbe
Article

Autophagy Proteins Promote Repair of Endosomal Membranes Damaged by the *Salmonella* Type Three Secretion System 1

Saskia Kreibich,[1] Mario Emmenlauer,[2] Jennifer Fredlund,[3] Pauli Rämö,[2] Christian Münz,[4] Christoph Dehio,[2] Jost Enninga,[3] and Wolf-Dietrich Hardt[1,*]
[1]Institute of Microbiology, ETH Zurich, Vladimir-Prelog Weg 4, 8093 Zurich, Switzerland
[2]Biozentrum, University of Basel, Klingelbergstrasse 50/70, 4056 Basel, Switzerland
[3]Dynamics of host-pathogen interaction Unit, Institut Pasteur Paris, 25-28 Rue du Docteur Roux, 75015 Paris, France
[4]Institute of Experimental Immunology, University of Zurich, Winterthurerstrasse 190, 8057 Zürich, Switzerland
*Correspondence: hardt@micro.biol.ethz.ch
http://dx.doi.org/10.1016/j.chom.2015.10.015

SUMMARY

Salmonella Typhimurium (*S*.Tm) is an enteropathogen requiring multiple virulence factors, including two type three secretion systems (T1 and T2). T1 triggers epithelium invasion in which the bacteria are taken up into endosomes that mature into *Salmonella*-containing vacuoles (SCV) and trigger T2 induction upon acidification. Mechanisms controlling endosome membrane integrity or pathogen egress into the cytosol are incompletely understood. We screened for host factors affecting invasion and SCV maturation and identified a role for autophagy in sealing endosomal membranes damaged by T1 during host cell invasion. *S*.Tm-infected autophagy-deficient (*atg5*$^{-/-}$) cells exhibit reduced SCV dye retention and lower T2 expression but no effects on steps preceding SCV maturation. However, in the absence of T1, autophagy is dispensable for T2 induction. These findings establish a role of autophagy at early stages of *S*.Tm infection and suggest that autophagy-mediated membrane repair might be generally important for invasive pathogens and endosomal membrane function.

INTRODUCTION

Salmonella enterica serovar Typhimurium (*S*.Tm) can cause diarrhea by infecting the gut tissue. This is facilitated by virulence factors, i.e., the type three secretion systems T1 and T2, which inject effector proteins and thereby manipulate host cell responses (Kaiser et al., 2012). However, the precise role of T1 and T2 in the pathogen-host interaction and the mechanisms maintaining host cell membrane integrity in face of T1 and T2 are not yet fully understood.

The T1 effector proteins SipA, SopE, SopE2, and SopB trigger actin rearrangements and epithelial cell invasion (Table S1A; Kaiser et al., 2012). Initially, *S*.Tm lodges in endosomes. In wild-type (WT) epithelial cells, most *S*.Tm remain in *Salmonella*-containing vacuoles (SCV), which sequentially acquire early (Rab5) and late (Rab7, Rab9, and Lamp1) endosomal markers, and acidify (thus triggering T2) but do not fuse with lysosomes (Bakowski et al., 2008; Smith et al., 2005; Yu et al., 2010). However, a small sub-fraction egresses from the SCV and grows at high rates in the host cell cytosol ("hyper-replication"; Knodler et al., 2010, 2014; Malik-Kale et al., 2012). It is still not completely understood how SCV egress and cytosolic hyper-replication are limited by the host cell.

Innate defenses allow mammalian cells to recognize and respond to bacteria (Fredlund and Enninga, 2014). This includes autophagy. Autophagy proteins promote cellular homeostasis by delivering cytosolic cargo to lysosomal degradation. Starvation, stress, and intracellular bacteria can induce autophagy (Huang and Brumell, 2014), trigger the uptake of cytosol- and phagophore-residing pathogens into autophagosomes, and target them for lysosomal pathogen elimination (Levine et al., 2011; Nakagawa et al., 2004; Shahnazari et al., 2011; Watson et al., 2012). Some pathogens can escape autophagic recognition (*L. monocytogenes*, *S. flexneri*) or subvert autophagy to their own benefit (*C. burnetii*, *F. tularensis*, *B. abortus*) (Baxt et al., 2013; Berón et al., 2002; Gutierrez et al., 2005; Ogawa et al., 2005; Romano et al., 2007; Starr et al., 2012; Yoshikawa et al., 2009). Thus, autophagy can impose important checkpoints for infection. However, the underlying mechanisms remain incompletely understood.

Autophagy can restrict *S*.Tm infections (Huang and Brumell, 2014). Most work employed bulk assays and thereby focused on T1-mediated SCV damage/egress, cytosolic hyper-replication, and the mechanisms activating autophagy. Ruptured SCVs are sensed by galectins, cytoplasmic lectins recognizing carbohydrate modifications within the ruptured SCV, which subsequently recruit adaptors and autophagosomes (Thurston et al., 2012). Moreover, autophagy targets cytoplasmic *S*.Tm for degradation (Thurston et al., 2009, 2012; Wild et al., 2011; Zheng et al., 2009). Thereby, dysfunctional autophagy leads to hyper-replication within the host cytoplasm (Birmingham et al., 2006; Kuballa et al., 2008; Tattoli et al., 2012). However, some contradictory evidence has been reported (Yu et al., 2014), and the precise role of autophagy in the infection is still not completely understood.

We employed an unbiased approach and a SCV-specific reporter to identify host cellular factors affecting the *S*.Tm infection

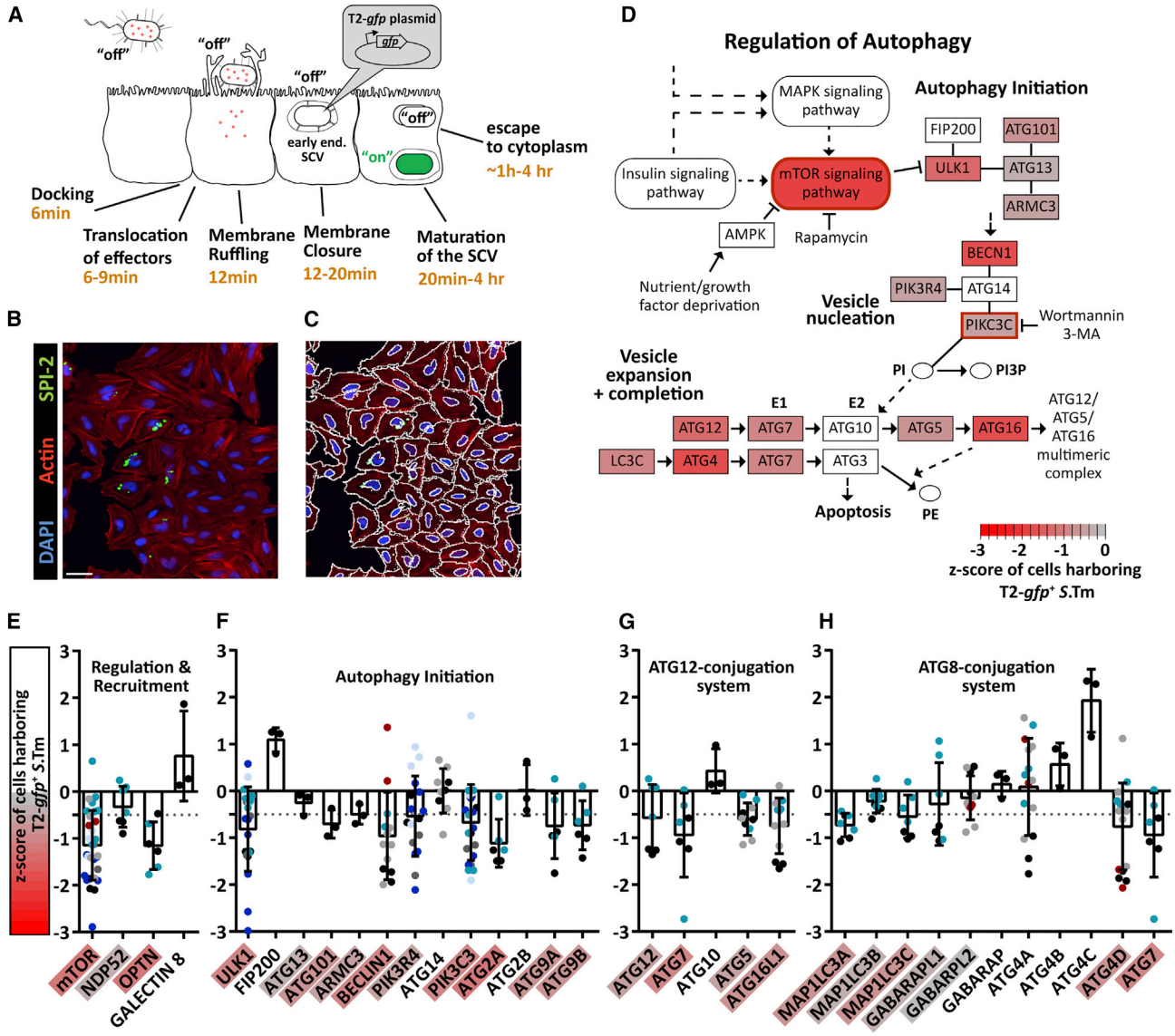

Figure 1. Genome-wide RNAi Screen Implicating Autophagy

(A) T2-*gfp* reporter assay (see Supplemental Information; Misselwitz et al., 2011a).

(B and C) Image-based screen of HeLa nuclei (DAPI), actin (DY-547 phalloidin), and T2-*gfp* expression. Bar, 10 μm. CellProfiler-based identification of nuclei, cell borders, and T2-*gfp*-expressing *S.*Tm^{SopE} (Supplemental Information).

(D) Results (data shown in Table S1B). Autophagy was identified by KEGG-pathway analysis (Luo and Brouwer, 2013) and phenotypic clustering of the 5,000 strongest hits. Red frames indicate hits from earlier work (Misselwitz et al., 2011a) and inhibitors.

(E–H) Knockdown phenotypes (*Z* scores) of autophagy hits from Table S1B. Dots indicate screen data (black, GWS; gray, Ambion; red, esiRNA; turquoise, QIAGEN; dark/light blue, Dharmacon pooled/unpooled); bar indicates mean with SD. Color code as in (D). Stippled line: cutoff = −0.5 *Z* score (≈30% attenuation). ATG7 is involved in ATG12 and ATG8 systems (G and H).

process. This revealed a role for autophagy in the repair of T1-mediated SCV membrane damage.

RESULTS

RNAi Screen Identifies Host Cell Factors Affecting *S.*Tm Infection

To identify host cell factors affecting *S.*Tm infection, we conducted a genome-wide RNAi screen (GWS), using the modified gentamicin-protection assay (termed *gfp*-reporter assay from here on) and *S.*Tm^{SopE}, as described (Figure 1A; Table S1A; Misselwitz et al., 2011a). *S.*Tm^{SopE} (SL1344, Δ*sopE2sip AsopB*), which strictly requires SopE for host cell invasion (Schlumberger and Hardt, 2006), carried p*ssaG*, a reporter plasmid expressing GFP from a T2 promotor (Schlumberger et al., 2007). Thus, GFP is induced only after invasion of the host cell, when the pathogen arrives in a properly matured SCV (Figure 1A; Figures S1A–S1D and S6; Supplemental Experimental Procedures). Automated microscopy and image analysis quantified the percentage of cells harboring T2-*gfp*$^+$ *S.*Tm.

Thereby, host cell factors affecting any step of the infection pathway leading to SCV maturation could be identified, i.e., binding, effector translocation, ruffling, internalization, and the maturation of the SCV (Figures S1A–S1D; Misselwitz et al., 2011a).

HeLa CCL-2 cells were transfected with a genome-wide siRNA library (Dharmacon ON-TARGETplus SMART pool; 18,237 target genes; three independent replicates), kinase/phosphatase-targeting, or customized siRNA libraries (Table S1B) and infected for 4 hr. Infection efficiencies were scored by an automated image analysis pipeline (1,000–3,500 cells/well; Figures 1B and 1C; Supplemental Experimental Procedures). Biological siRNA controls (Kif11, ArpC3, Cdc42) served as controls to verify plate quality and high inter-screen reproducibility (R^2 = 0.8–0.9; data not shown; Misselwitz et al., 2011a; Figures S1E and S1F).

Phenotypic clustering and mapping of the 5,000 strongest hits (Z score ≤ -0.5; i.e., $\geq$ 30% attenuation) onto KEGG pathways identified signaling modules of interest. This rediscovered actin cytoskeleton regulators (e.g., Rac1, Cdc42, N-WASP, CYFIP2, NCKAP1, ABI2, WAVE2, Arp2/3 proteins, PFN; Figure S1G), the COPI complex (Misselwitz et al., 2011a), the trafficking GTPases Rab5 and Rab7, and the vacuolar ATPases promoting SCV acidification and T2 induction (Rathman et al., 1996; Table S1B). Strikingly, we also identified numerous strong autophagy hits affecting regulation and recruitment, autophagy initiation, and the ATG12- or the ATG8-conjugation system (Figures 1D–1H). Their silencing had only minor effects on the cell numbers (<<2-fold; Table S1B), and this effect did not affect our readout (data not shown). Some autophagy proteins (e.g., ATG10, ATG13, FIP200) did not yield significant phenotypes. Most likely, this is explained by inefficient knockdown and/or masking by positive off-target effects (Franceschini et al., 2014). The ATG8-conjugation system yielded only subtle effects on *S*.Tm infection. It seems likely that this is explained by functional redundancy. Overall, however, silencing of most autophagy proteins reduced the number of cells harboring T2-*gfp*-expressing *S*.Tm. This phenotype was apparently at odds with the established role of autophagy in restricting cytosolic pathogen growth (Birmingham et al., 2006; Figures S2A and S2B), and it was not explained by autophagy-controlled pathogen expulsion (Figures S2E and S2F). Thus, autophagy may have an additional function in the infection process that had not been discovered so far.

atg5-Deficient Murine Fibroblasts Verify the Need for Autophagy in SCV Maturation

Mouse embryonic fibroblasts (MEFs) and an *atg5*$^{-/-}$ mutant (Kuma et al., 2004) were used to decipher the role of autophagy in SCV maturation and T2 induction. ATG5, ATG12, and ATG16L1 form an E3-ubiquitin ligase of the ATG8-conjugation system involved in autophagosome elongation and closure (Fujita et al., 2008; Hanada et al., 2007; Mizushima et al., 2001, 2003). When infected with *S*.Tm^{SopE}, T2-*gfp* expression was reduced by 50% in the *atg5*$^{-/-}$ cells ($p << 0.05$; Figure 2A). Equivalent data were obtained in infections with WT (*S*.Tm; Figure S2G) or *S*.Tm^{SipA}, an isogenic mutant invading via SipA (data not shown). This confirmed that the *atg5* phenotype is not limited to *S*.Tm^{SopE}, but of general relevance for *Salmonella* host cell infection.

Infection Steps Preceding Endosome/SCV Maturation Do Not Require *atg5*

Infection-stage-specific assays were used to map the effect of *atg5* deficiency. Docking, as measured by infecting *atg5*$^{-/-}$ and *atg5*$^{+/+}$ MEFs for 6 min with *S*.Tm$^{\Delta 4}$ (lacks *sopE*, *sopE2*, *sopB*, *sipA*; docks via T1 and type I fimbriae; Misselwitz et al., 2011b) did not differ significantly between *atg5*$^{-/-}$ and *atg5*$^{+/+}$ MEFs ($p \geq 0.05$; Figure 2B). Equivalent observations were made in HeLa CCL-2 cells (log2 docking index 0.5 to −0.5; Figure S2I). Also, membrane ruffling, as analyzed 12 min post-infection (p.i.) with *S*.Tm^{SopE}, did not differ between *atg5*$^{-/-}$ and *atg5*$^{+/+}$ MEFs ($p \geq 0.05$; Figure 2C; Supplemental Experimental Procedures). Finally, at 1 hr p.i., a classical gentamicin-protection assay yielded equivalent levels of *S*.Tm^{SopE} host cell invasion in *atg5*$^{-/-}$ and *atg5*$^{+/+}$ MEFs ($p > 0.05$; Figure 2D). Thus, autophagy does not affect the steps preceding endosome/SCV maturation.

Different Kinetics of Autophagy-Promoted T2 Induction and Cytosolic Hyper-replication

To delineate the onset of autophagy-promoted SCV maturation, *atg5*$^{-/-}$ and *atg5*$^{+/+}$ MEFs were infected for 1–12 hr with *S*.Tm^{SopE} (Figure 2E). T2-*gfp* was expressed as early as 2 hr p.i., and *atg5*$^{-/-}$ cells revealed reduced induction levels ($p < 0.05$; Figure 2E). Equivalent observations were made in WT *S*.Tm (Figure S2G).

In contrast, a classical gentamicin-protection assay yielded the well-described hyper-proliferation in *atg5*$^{-/-}$ cells. This assay detects all intracellular (sum of T2-*gfp*$^{+}$ and T2-*gfp*$^{-}$) *S*.Tm. As expected, the phenotype appeared later, i.e., by $\geq$ 4 hr p.i. (Birmingham et al., 2006; Figure 2F; Figures S2A and S2B). After 5–6 hr, *atg5*$^{-/-}$ (but not the *atg5*$^{+/+}$) cells showed massive intracellular pathogen growth (Figure 2G; Brumell et al., 2002; Knodler et al., 2010, 2014; Malik-Kale et al., 2012). This was confirmed by fluorescence microscopy (Figures S2J and S2K). Thus, cytoplasmic hyper-proliferation (at $\geq$ 4 hr p.i.) begins about 2 hr later than the autophagy-promoted SCV maturation (1–2 hr p.i.). Moreover, T2-*gfp*$^{+}$ *S*.Tm were still observable in *atg5*$^{-/-}$ cells harboring massive amounts of hyper-proliferating (T2-*gfp*$^{-}$) bacteria (Figure 2H). This suggested that the effect of autophagy on SCV maturation/T2 induction is functionally distinct and can be studied specifically using the T2-*gfp* reporter assay.

Interdependence of Autophagy and Endosome-to-SCV Maturation

To assess the interplay between autophagy, the endosome system, and T2 induction, we infected *atg5*$^{-/-}$ and *atg5*$^{+/+}$ MEFs expressing markers for early (Rab5-RFP) or late endosomes (Rab7-RFP) or for lysosomes (Lamp1-RFP) for 2 or 4 hr with *S*.Tm^{SopE}. While *atg5*$^{-/-}$ cells harbored reduced numbers of T2-*gfp*-expressing *S*.Tm^{SopE} (Figure 2A, data not shown), the Rab5 and Lamp1 association with the remaining T2-*gfp*-expressing bacteria did not differ in *atg5*$^{-/-}$ versus *atg5*$^{+/+}$ MEFs ($p \geq 0.05$; Figures 3A and 3C). Similar observations were made with respect to Rab7, except for a slight difference at 4 hr p.i. (Figure 3B). Finally, bafilomycin-mediated inhibition of endosome acidification reduced T2-*gfp* induction in both *atg5*$^{-/-}$ and *atg5*$^{+/+}$ MEFs by > 10-fold (Figure S3A). Overall,

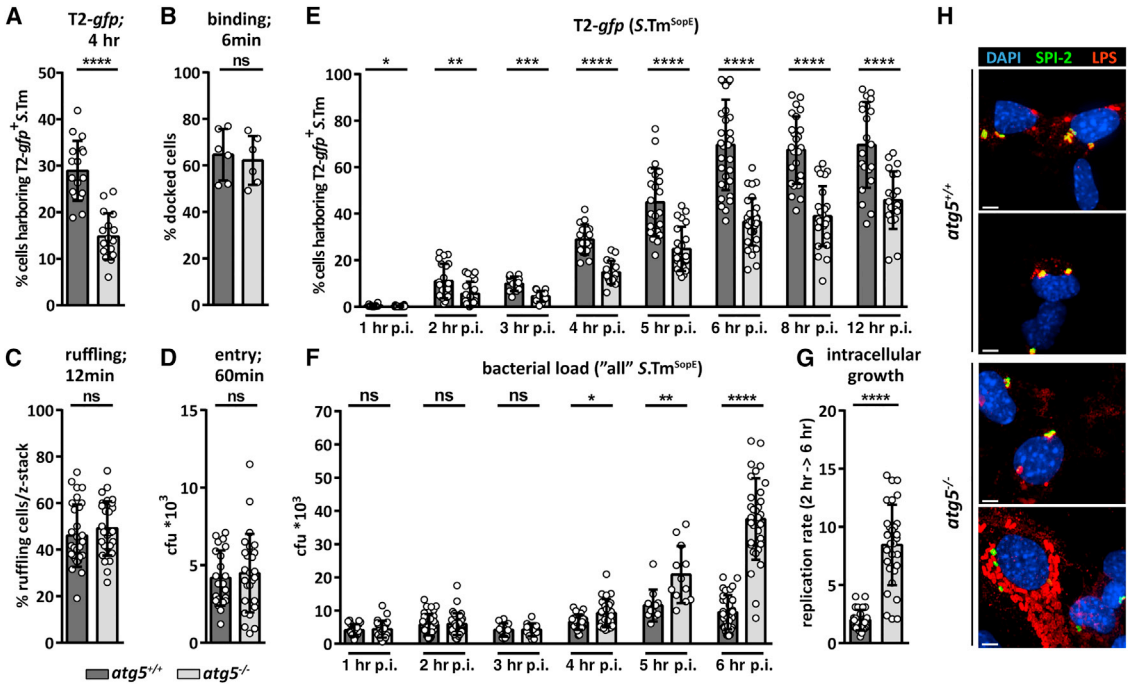

Figure 2. Impact of *atg5* on Distinct Stages of *S*.Tm Infection

(A) T2-*gfp* expression at 4 hr p.i. of *atg5*$^{+/+}$ (dark) or *atg5*$^{-/-}$ (light gray) MEFs with *S*.Tm^{SopE} (MOI = 60).

(B) Binding of *S*.Tm$^{\Delta 4}$ (MOI = 125; 6 min p.i.).

(C) Ruffling triggered by *S*.Tm^{SopE} (MOI = 80; 12 min p.i.; 571 or 549 cells analyzed).

(D) Gentamicin-protection assay (*S*.Tm^{SopE} CFU; 1 hr p.i.; MOI = 10).

(E) Time course of *S*.Tm^{SopE} infection (T2-*gfp* assay; 1–12 hr p.i.; MOI = 40).

(F) Gentamicin-protection time course assay (*S*.Tm^{SopE} CFU; MOI = 10).

(G) Intracellular growth ([CFU (6 hr p.i.)] / [CFU (2 hr p.i.)]); data from (F).

(H) Fluorescence microcopy of *atg5*$^{+/+}$ or *atg5*$^{-/-}$ MEF 6 hr p.i. with *S*.Tm^{SopE}. Red, α-LPS-CY5 ("all *S*.Tm"); green, T2-*gfp*; blue, DAPI. Bar indicates 5 μm. All data were from ≥ 5 independent replicates (whisker bar indicates mean and SD).

these data suggest that *atg5*-dependent and *atg5*-independent SCV maturation proceed along similar pathways.

Effects on SCV egress and cytosolic proliferation were assessed by quantifying Rab5, Rab7, and Lamp1 association with all *S*.Tm (carrying a constitutive reporter). As expected, when most bacteria lodge in intact SCV, the *atg5*$^{+/+}$ data for all *S*.Tm were quite similar to those obtained for T2-*gfp*$^{+}$-expressing *S*.Tm (compare Figures 3A–3C to Figures 3D–3F). In *atg5*$^{-/-}$ cells, all *S*.Tm showed reduced Rab7 and Lamp1 association by 4 hr p.i. This is consistent with SCV escape and cytoplasmic hyper-proliferation. Interestingly, the Rab7 and Lamp1 association was already reduced by 2 hr p.i. (Figures 3E and 3F), a time point preceding the cytoplasmic hyper-proliferation (Figures 2F and 2G; Figures S2J and S2K). Thus, SCV egress might occur already by 2 hr p.i. in *atg5*$^{-/-}$ cells, and cytoplasmic bacteria might undergo a lag phase of 1–2 hr before hyper-replication commences.

To test the effect of SCV maturation defects on egress, we infected *atg5*$^{-/-}$ and *atg5*$^{+/+}$ MEFs expressing WT, constitutively active (CA), or dominant-negative (DN) Rab7-GFP mutants. As expected (Harrison et al., 2004), the DN Rab7 failed to co-localize with bacteria in WT and mutant MEF (Figure S3B). In contrast, CA Rab7 was recruited to all *S*.Tm with a higher efficiency than WT Rab7. However, even CA Rab7 was recruited with reduced efficiency in *atg5*$^{-/-}$ MEFs. Thus, Rab7 activation is needed to recruit Rab7 to the SCV, but Rab7 activation cannot bypass the SCV maturation defect of *atg5*$^{-/-}$ cells.

Finally, we analyzed if Rab5 knockdown affects LC3 association with intracellular *S*.Tm. Supported by previous findings (Smith et al., 2007), combinatorial Rab5A/B/C knockdown reduced T2-*gfp* induction (Figure S3C). Moreover, the knockdown had minor effects at best on the LC3 recruitment to all *S*.Tm (Figure S3D). Thus, Rab5A/B/C contributes to the initial stages of SCV maturation, but seems dispensable for LC3 recruitment to leaky SCV and/or cytoplasmic *S*.Tm.

T2-Function Is Dispensable for Induction of the T2-*gfp* Reporter

T2 is well known to manipulate host cellular vesicle traffic (Figueira and Holden, 2012). To test if this activity contributes to T2-*gfp* induction, we infected *atg5*$^{-/-}$ and *atg5*$^{+/+}$ MEFs with *S*.Tm$^{\Delta T2}$ (SL1344 *sseD::aphT*). T2-*gfp* induction kinetics did not differ significantly between *S*.Tm$^{\Delta T2}$, *S*.Tm^{SopE}, and WT *S*.Tm (compare Figure 4 to Figure 2E and Figure S2G). Thus, a functional T2 system does not further promote T2 induction. Rather, T2 appears to be induced by environmental cues (i.e., vacuolar acidification; Figure S3A) emanating from the host cellular

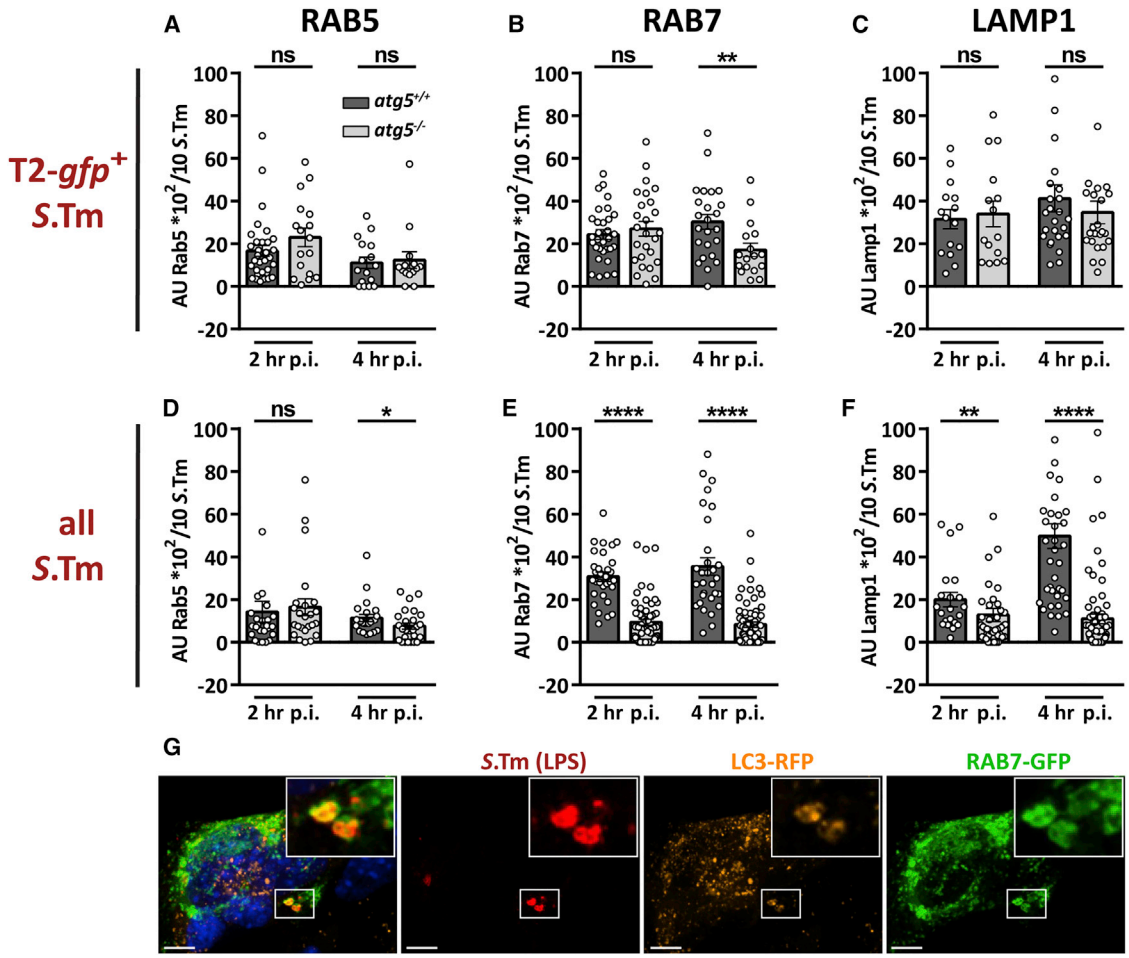

Figure 3. Endosome Marker Localization to *S*.Tm^{SopE} in WT or *atg5*$^{-/-}$ MEFs

(A–F) MEFs transfected with endosome reporters as indicated and analyzed at 2 or 4 hr p.i. with *S*.Tm^{SopE} (MOI = 40; Volocity quantitation module). Association of Rab5 (A), Rab7 (B), and Lamp1 (C) to T2-*gfp*$^{+}$ *S*.Tm^{SopE} in *atg5*$^{+/+}$ and *atg5*$^{-/-}$ MEFs is shown. Association of Rab5 (D), Rab7 (E), and Lamp1 (F) to *S*.Tm^{SopE} expressing constitutive GFP in *atg5*$^{+/+}$ and *atg5*$^{-/-}$ MEFs is also shown. All data were from ≥ 2 independent experiments. Circles indicate average fluorescence (AU, arbitrary unit) around ten randomly picked *S*.Tm (mean and SEM).

(G) Representative fluorescence microscopy image of *atg5*$^{+/+}$ MEFs at 2 hr p.i. with *S*.Tm^{SopE}. Orange, stable LC3-RFP; green, transiently expressed Rab7-GFP; red, α-LPS-CY5 antibody staining all *S*.Tm^{SopE}. Bar, 5 μm.

endosome-to-SCV maturation process, at least during the first 6 hr of infection, in murine fibroblasts.

In the Absence of T1, *atg5* Is Dispensable for T2 Induction

So far, it had remained unclear why autophagy promotes T2 expression. T1 can elicit SCV damage, transiently induce autophagy (by ≈1 hr p.i.) and initiate the restriction of cytosol-exposed *S*.Tm (Birmingham et al., 2006; Ivanov and Roy, 2009; Tattoli et al., 2012). To test if the autophagy-promoted T2 induction originates from T1-inflicted membrane damage, *atg5*$^{-/-}$ and *atg5*$^{+/+}$ MEF were infected with *S*.Tm$^{\Delta T1}$ (SL1344, Δ*invG*; T1 defective; Table S1A). *S*.Tm$^{\Delta T1}$ internalization was promoted by co-infection with *S*.Tm^{SopE} (the helper strain at a 1:5 mixture with *S*.Tm$^{\Delta T1}$pT2-*gfp*; Birmingham et al., 2006; Misselwitz et al., 2011a; Steele-Mortimer et al., 2002). Lamp1 staining suggested that *S*.Tm$^{\Delta T1}$ and *S*.Tm^{SopE} do generally reside in separate SCVs (Figures S4A–S4C). Intriguingly, the time course of T2-*gfp* expression by *S*.Tm$^{\Delta T1}$ (Figure 5A) was similar to that of *S*.Tm^{SopE} (Figure 2E), but did not differ between *atg5*$^{-/-}$ and *atg5*$^{+/+}$ cells ($p \geq 0.05$). Moreover, plating indicated that *S*.Tm$^{\Delta T1}$ did not grow intracellularly, neither in *atg5*$^{-/-}$ nor in *atg5*$^{+/+}$ cells for 6 hr p.i. ($p \geq 0.05$; Figures 5B and 5C). This suggested that, even in the absence of autophagy, *S*.Tm$^{\Delta T1}$ remained in a vacuolar compartment and therefore did not engage in cytosolic hyper-replication (Figures S2C and S2D). Equivalent data were obtained when internalization of *S*.Tm$^{\Delta T1}$ was driven by a plasmid expressing invasin (Figures S4D–S4F), a well-characterized adhesin from *Yersinia pseudotuberculosis* (Hardt et al., 1998; Isberg and Van Nhieu, 1995; Isberg et al., 1987). Taken together, these data imply that T1-inflicted SCV damage elicits not only the tagging and elimination of cytosol-exposed bacteria (Braun et al., 2010; Malik-Kale et al., 2012; Mallo et al., 2008), but also the sealing of the damaged SCV, which promotes T2 induction.

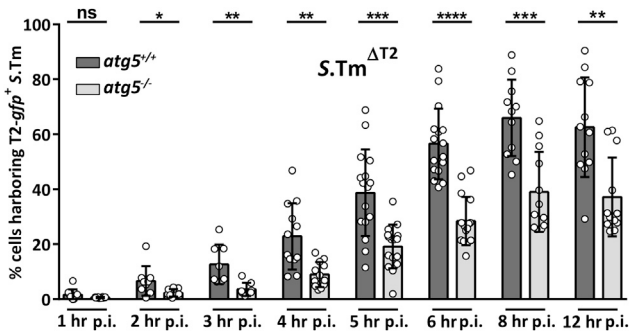

Figure 4. Time Course of SCV Maturation in *S*.Tm$^{\Delta T2}$-Infected Cells

atg5$^{+/+}$ or *atg5*$^{-/-}$ MEFs were infected with *S*.Tm$^{\Delta T2}$ (T2-*gfp* assay [1–12 hr p.i.; MOI = 40]). Data were from ≥ 6 independent experiments (dots, data point; whisker bar, mean and SD).

LC3 Is Recruited in a T1-Dependent Fashion

To establish the kinetics of T1-mediated autophagy induction, we analyzed the time course of LC3 recruitment. LC3 is recruited and conjugated in an ATG5-dependent fashion to *S*.Tm lodged in ruptured endosomes or the host cell cytosol (Birmingham et al., 2006; Fujita et al., 2008; Hanada et al., 2007). In *S*.Tm^{SopE}-infected WT (but not *atg5*$^{-/-}$) MEFs, LC3 was recruited as early as 40 min p.i., peaked at 40–60 min, and declined by 90–240 min p.i. (Figures 6A and 6B). In contrast, helped invasion of *S*.Tm$^{\Delta T1}$ (helper = *S*.Tm^{SopE}) did not yield any LC3 recruitment, neither in the *atg5*$^{-/-}$ nor the *atg5*$^{+/+}$ cells (Figures S5A and S5B). These data verified that autophagy is activated already at early stages after invasion by T1-positive bacteria, while T1-deficient bacteria do not activate this host cellular response.

Interestingly, some internalized *S*.Tm^{SopE} cells acquired LC3, while others did not (Figure 6A). We speculated that this is attributable to the bimodal T1 expression of *S*.Tm (Hautefort et al., 2003; Saini et al., 2010; Schlumberger et al., 2005; Sturm et al., 2011; Winnen et al., 2008). Thereby, the inoculum of WT *S*.Tm or *S*.Tm^{SopE} harbors about 30% of T1-expressing cells (T1-on) and 70% T1-off cells. Only the T1-on bacteria trigger membrane ruffles (and inflict T1 damage; should lead to transient LC3 recruitment and repair or to egress), while T1-off bacteria enter passively (i.e., like *S*.Tm$^{\Delta T1}$ in Figure 5). When we infected *atg5*$^{+/+}$ cells (*atg5*$^{-/-}$ = neg. control) for 40 min with *S*.Tm^{SopE}, the LC3 recruitment to the average invading bacterium was significantly higher at MOI = 1 than at MOI = 10 ($p < 0.05$; Figure 6C). Similarly, in infections with *S*.Tm^{SopE} (T2-*gfp* reporter, MOI = 1), the LC3 recruitment to the bacteria was strikingly similar between T2-*gfp*$^{+}$ and all bacteria (constitutive reporter; $p > 0.05$; Figure 6D). Similar observations were made with recruitment of Galectin-3, a cytosolic danger receptor (Figures S5C–S5E). These data provided further support that T1 inflicts endosome damage and that autophagy promotes its repair, thereby fostering endosome-to-SCV maturation and T2 induction.

Fluid-Phase Marker Retention Confirmed the Role of Autophagy in SCV Repair

To verify delayed endosome repair in the autophagy-deficient cells, *atg5*$^{-/-}$ and *atg5*$^{+/+}$ MEFs were incubated with FITC-

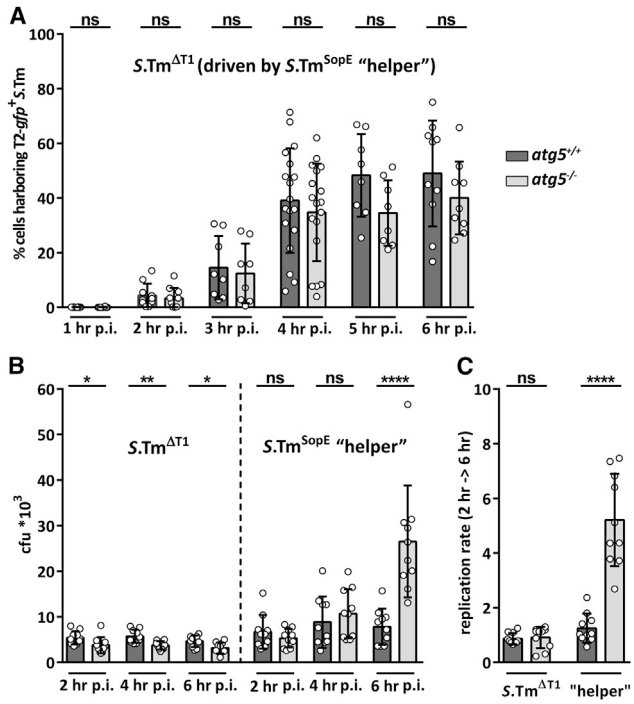

Figure 5. Time Course of SCV Maturation in *S*.Tm$^{\Delta T1}$-Infected Cells

(A) *atg5*$^{+/+}$ or *atg5*$^{-/-}$ MEFs were infected with a mixture of *S*.Tm^{SopE} ("helper"; trigger ruffles; no *gfp* plasmid; MOI = 40–60) and *S*.Tm$^{\Delta T1}$ (T2-*gfp* reporter; MOI = 150–250). T2-*gfp* expression was analyzed as above (Figure 2E). Data were from ≥ 6 independent experiments.

(B) Gentamicin-protection assay time course with a mixture of *S*.Tm^{SopE} ("helper"; no *gfp* plasmid; MOI = 8) and *S*.Tm$^{\Delta T1}$ (T2-*gfp* reporter; MOI = 40). Pathogen loads were determined by plating.

(C) Intracellular growth ([CFU (6 hr p.i.)]/[CFU (2 hr p.i.)]); data from (B). Dots, data points; whisker bar, mean and SD.

dextran (500 kDa) and infected for 90 min with *S*.Tm^{SopE}. FITC-dextran retention in SCVs was more pronounced in *atg5*$^{+/+}$ than in *atg5*$^{-/-}$ cells ($p < 0.05$; Figure 7A). No such difference was observed in *S*.Tm$^{\Delta T1}$ infections ($p \geq 0.05$; helper = *S*.Tm^{SopE}). We also quantified FITC-dextran retention in SCVs showing evidence of membrane damage. Galectin-3-mOrange-expressing *atg5*$^{-/-}$ and *atg5*$^{+/+}$ MEFs were infected for 90 min with *S*.Tm^{SopE}. Galectin-3-positive SCVs yielded lower FITC-dextran signals than the average SCV, both in the *atg5*$^{-/-}$ and the *atg5*$^{+/+}$ cells (Figure 7A). This confirmed that T1 compromises SCV integrity and that autophagy supports the sealing of damaged SCV membranes.

Finally, we analyzed the effect of osmotic shock-inflicted membrane damage. *atg5*$^{-/-}$ and *atg5*$^{+/+}$ MEFs expressing Galectin-3-mOrange were treated with Blue-dextran (500 kDa) and HGF to allow internalization of *S*.Tm$^{\Delta T1}$ (constitutive *gfp*). We inflicted membrane damage (10 min, 0.5 M sucrose + 10% PEG1000 followed by 3 min in 60%PBS) and analyzed dye-dextran retention in the vicinity of *gfp*-expressing bacteria. Osmotic shock slightly reduced dye-dextran retention in *atg5*$^{+/+}$ controls (Figures 7B and 7C). More pronounced loss of dye-dextran retention was observed in *atg5*$^{-/-}$ cells. This may suggest a general role for autophagy in maintaining endosome membrane integrity.

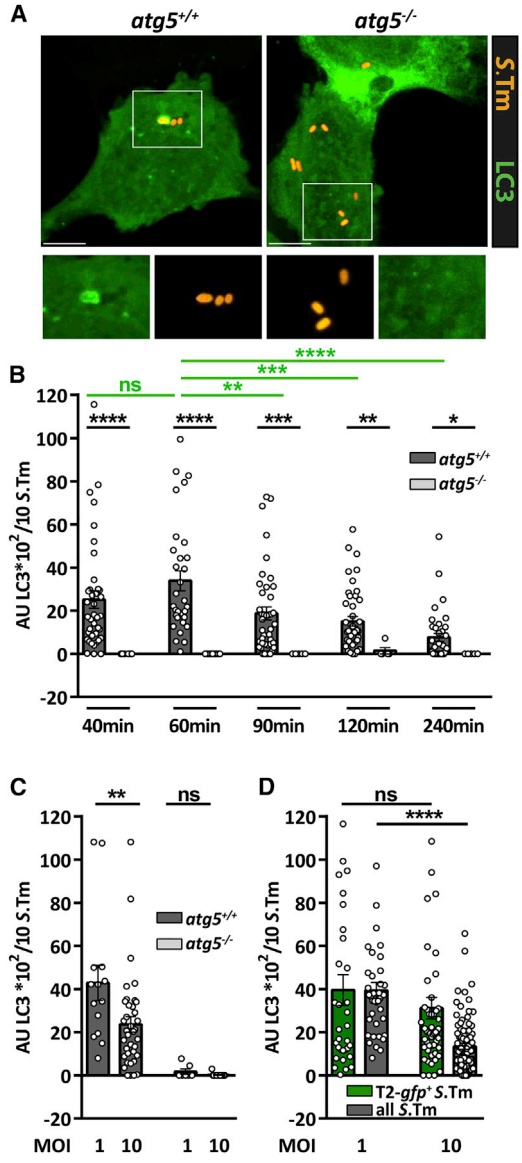

Figure 6. Impact of Autophagy on the T1-Expressing *S*.Tm Subpopulation

(A) Representative images of *atg5*$^{+/+}$ or *atg5*$^{-/-}$ MEFs stably expressing LC3-GFP at 40 min p.i. with *S*.Tm^{SopE} (constitutive mCherry; MOI ≈30); bar, 10 μm.

(B) Time course of LC3-GFP recruitment to *S*.Tm^{SopE} (constitutive mCherry; 40–240 min p.i.; MOI ≈30).

(C) LC3-GFP recruitment to *S*.Tm^{SopE} at MOI = 1 or 10 (constitutive mCherry; 40 min p.i.).

(D) LC3-RFP recruitment in *atg5*$^{+/+}$ MEFs to *S*.Tm^{SopE} at MOI = 1 or 10 at 2 hr p.i. Green, data for T2-*gfp* expressing *S*.Tm^{SopE}; gray, data for *S*.Tm^{SopE} expressing constitutive GFP. Data are from ≥ 2 independent experiments. Dots, average LC3 fluorescence (AU, arbitrary unit) per ten *S*.Tm; whisker bar, mean and SEM.

DISCUSSION

Our study identified a function for autophagy during repair of T1-inflicted SCV damage at the early stages of *S*.Tm infection. This fosters SCV maturation and thereby promotes T2 induction (see working model; Figure 7D), which is distinct from the well-described function of autophagy in tagging ruptured endosomes and lysosomal killing of cytosolic *S*.Tm (Birmingham et al., 2006; Tattoli et al., 2012; Thurston et al., 2012). Thus, autophagy controls two different effector mechanisms during infection. Both mechanisms are needed to confine the majority of the invading *S*.Tm cells to the SCV and thereby promote T2 expression by the vast majority of internalized bacteria.

SCV membrane sealing seems to require regulators (mTOR), recruitment factors (galectins, Optineurin), and initiation factors (ULK1, PI3-kinase C3, Beclin1, ATG2A, ATG9) as well as the ATG12- (ATG5, ATG7, ATG12, ATG16L1) and ATG8-conjugation systems. Individual elements (MAP1LC3A, MAP1LC3B, MAP1LC3C, GABARAPL1, GABARAPL2, and GABARAP) of the ATG8-conjugation system had only mild effects at best, which is likely attributable to functional redundancy. LC3 recruitment to *S*.Tm is thought to occur through the canonical autophagy pathway involving ULK1, Beclin1, and ATG9 or through LC3-associated phagocytosis (LAP), requiring diacylglycerol (Shahnazari et al., 2010) and protein kinase Cδ (PKCδ)-mediated activation of NADPH oxidase and reactive oxygen species (ROS) (Fontayne et al., 2002; Huang et al., 2009). Autophagy-dependent SCV repair required ULK1, Beclin1, and ATG9 (Figure 1), suggesting that LC3 is recruited to the damaged SCV by canonical autophagy, not by LAP.

Three lines of evidence exclude that cytoplasmic hyper-replication in autophagy-deficient cells affects our assessment of T2 expression by SCV-lodged bacteria: (1) the diminished T2 induction was concurrent with the onset of the T2-*gfp* reporter expression (Figure 2E; 1–3 hr p.i); (2) this preceded the onset of cytosolic *S*.Tm growth, which became apparent only much later (4–6 hr p.i.; Figure 2F); and (3) the T2-*gfp* expression kinetics by *S*.Tm$^{\Delta T1}$ (which remains in the SCV even in *atg5*$^{-/-}$ cells) were not affected by the cytoplasmic hyper-proliferation of the reporter-less helper strain *S*.Tm^{SopE} (Figure 5C). Thus, both autophagy-dependent effector mechanisms can operate in parallel, and cytoplasmic hyper-replication does not interfere with the membrane sealing and T2 expression by SCV-lodged *S*.Tm.

It is interesting to note that T1 is not only driving invasion of epithelial cells and fibroblasts, but also the prime cause for endosomal membrane damage. Thus, the T1-expressing bacteria rely on a host cellular system (i.e., autophagy) to initiate repair of this membrane damage before the SCV can mature further, acidify, and allow the expression of T2. Strikingly, the T1-deficient bacteria (invading by helper-triggered ruffling or by invasin expression) can bypass this need for autophagy as they do not cause endosome membrane damage. This latter phenomenon may be of relevance for the WT *S*.Tm infection, as WT *S*.Tm forms 30% T1-expressing and 70% non-expressing bacterial cells (Ackermann et al., 2008; Diard et al., 2013; Hautefort et al., 2003; Schlumberger et al., 2005; Sturm et al., 2011). The T1-on bacteria require autophagy-promoted SCV repair, while the T1-off bacteria are entering by helped invasion, do not compromise SCV integrity, and thus bypass this need for autophagy. This is a striking example of an intricate pathogen-host interaction whereby the pathogen (i.e., the T1-on bacteria) relies on specific host responses in order to maintain an intracellular niche and coordinate virulence factor expression.

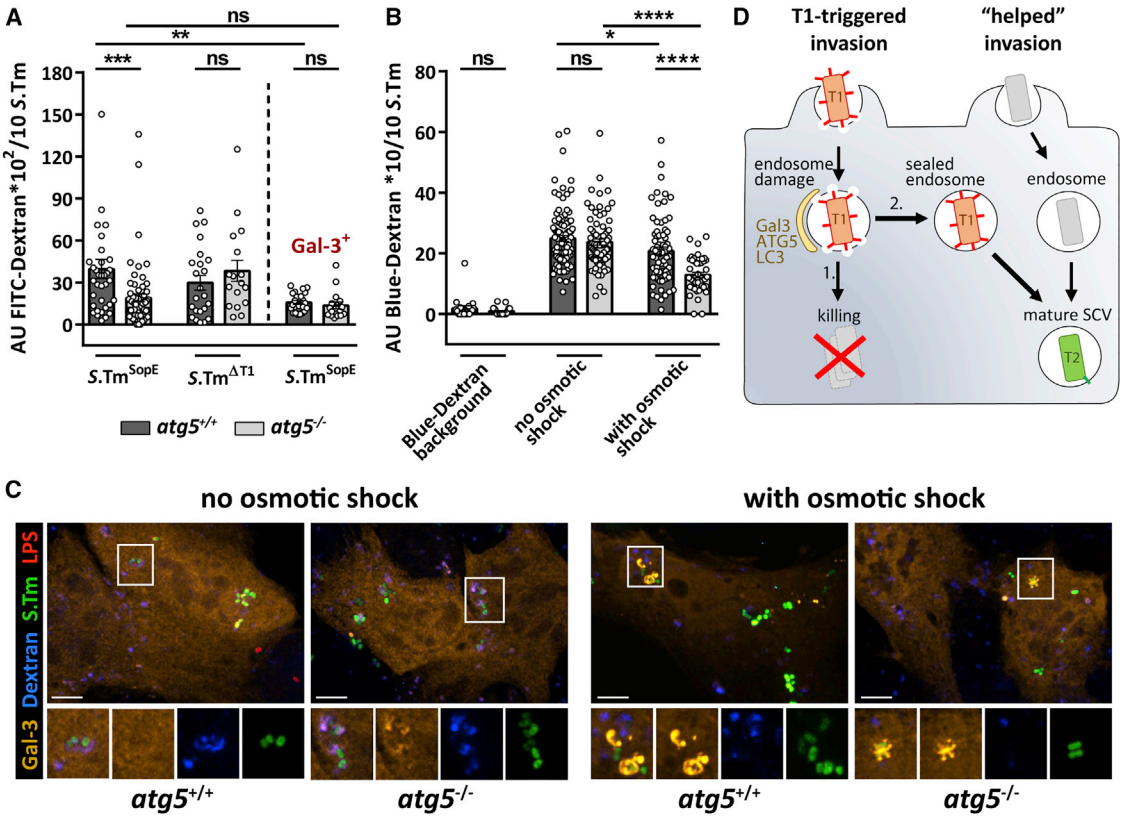

Figure 7. Fluid-Phase Marker Retention in the SCV

(A) *atg5*$^{+/+}$ or *atg5*$^{-/-}$ MEFs were incubated with 500 kDa FITC-dextran during a 90 min infection with *S*.Tm^{SopE} (constitutive mCherry; MOI = 40) or *S*.Tm$^{\Delta T1}$ (constitutive mCherry, MOI = 150; unlabeled helper strain = *S*.Tm^{SopE}). The FITC-dextran signal surrounding *S*.Tm^{SopE} or *S*.Tm$^{\Delta T1}$ was quantified. Right side: same as left side, but using Gal3-mOrange-expressing MEFs and α-LPS staining to detect *S*.Tm^{SopE}.

(B) Osmotic shock assay. *atg5*$^{+/+}$ or *atg5*$^{-/-}$ MEFs expressing Gal3-mOrange were incubated with 500 kDa Blue-dextran during a 90 min infection with *S*.Tm$^{\Delta T1}$ (constitutive GFP) internalized via HGF treatment. No infection = background; osmotic shock was inflicted after 57 min, i.e., by 10 min 0.5 M sucrose (PBS, 10% PEG1000), 3 min in 60% PBS, and 20 min recovery in culture media. The Blue-dextran signal surrounding *S*.Tm$^{\Delta T1}$ was quantified. Extracellular *S*.Tm$^{\Delta T1}$, identified by α-LPS antibodies, were excluded from analysis. Data are from ≥ 3 independent experiments. Dots, average dextran fluorescence (AU, arbitrary unit) per 10 *S*.Tm; whisker bar, mean and SEM.

(C) Representative images from (B). Bar, 10 μm.

(D) Model depicting the role of autophagy in promoting repair of T1-damaged endosome membranes. Red, T1-expressing *S*.Tm; gray, *S*.Tm without T1 expression; green, T2 expression; yellow, autophagy proteins.

The cellular processes sealing the damaged SCV membrane remain to be established. Clearly, the ATG12-conjugation system is involved and thereby promotes SCV maturation, vacuolar acidification, T2 expression, and the secretion of SPI-2 effectors to facilitate downstream events of the infection process. In the absence of functional autophagy, the dynamics of SCV repair are impaired and stall the compromised SCVs in a Rab5-positive stage, which is prone to bacterial egress and subsequent hyperproliferation at cytosolic sites later during infection.

Some evidence suggests that autophagy is of relevance for the infection in vivo. Enterocyte-specific ablation of *atg5*, *atg16L1*, or *atg7* in mice affected mucosal inflammatory responses and rendered the animals prone to systemic pathogen dissemination by *S*.Tm (Benjamin et al., 2013; Conway et al., 2013) and other enteric pathogens (Marchiando et al., 2013). However, the exact role of autophagy and the relative contribution of SCV repair, cytoplasmic pathogen elimination, or undiscovered effector functions remains to be established. One might speculate if some *Salmonella* strains may express virulence factors manipulating such responses. Up to date, RavZ from *Legionella pneumophila* is the only bacterial effector known to manipulate autophagy, i.e., by irreversibly deconjugating LC3 from the surface of pre-autophagosomal membranes (Amer and Swanson, 2005; Choy et al., 2012).

In the past years, there has been accumulating evidence suggesting that autophagy can affect pathogen traffic in different ways. In case of *Brucella abortus*, the pathogen-containing vacuole matures into a reticulum-like compartment (BCV) fostering pathogen replication. In this case, pathogen release from the infected cell requires the recruitment of autophagy initiation factors like ULK1 and Beclin1 to the BCV, while autophagy-elongation proteins (e.g., ATG5, ATG16L1, ATG4B, ATG7, and LC3B) were not needed (Starr et al., 2012). By contrast, the *Coxiella*-containing vacuole is decorated with LC3 throughout all intracellular phases of the infection, which is thought to delay the fusion with lysosomes (Berón et al., 2002; Gutierrez et al., 2005;

Romano et al., 2007). These cases are yet clearly different from the role of autophagy in *S*.Tm infection. Our findings of autophagy-dependent repair of SCVs harboring the T1-expressing *Salmonella* population in infected cells extend the mechanisms that are subverted by bacterial pathogens and emphasize the central role of autophagy in the pathogen-host cell interaction.

It has become clear that autophagy not only affects the handling of intracellular pathogens, but also sterile endosomes not harboring any bacteria (Thurston et al., 2012). In fact, endosome membrane defects in non-infected cells are efficiently tagged by Galectin-3, -8, and -9 (but not by Galectin-1; Thurston et al., 2012). Our osmotic shock data (Figures 7B and 7C) suggest that this might initiate endosome membrane repair. It will be interesting to find out if autophagy-mediated endosome membrane repair is of general importance for maintaining the endosomal membrane integrity in mammalian cells.

EXPERIMENTAL PROCEDURES

Cells and Plasmids

WT *S*.Tm (SL1344; Hoiseth and Stocker, 1981); *S*.Tm^{SopE} (SL1344, Δ*sopE2-sopBsipA*, M2421/M701; Hoffmann et al., 2010; Müller et al., 2009); *S*.Tm^{SipA} (SL1344, Δ*sopEsopE2sopB*, M516; Mirold et al., 2001); *S*.Tm$^{\Delta T1}$ (SL1344, Δ*invG*, SB161; Kaniga et al., 1994); *S*.Tm$^{\Delta T2}$ (SL1344, Δ*sseD*, M556; Hapfelmeier et al., 2004); HeLa CCL-2 cells; *atg5*$^{+/+}$ and *atg5*$^{-/-}$ mouse embryonic fibroblasts; the plasmids pM965, pM975, and pWRG435; and the expression constructs for WT and mutant forms of Rab5A, Rab7, Lamp1, Galectin-3, lentiviral transduction, and transient transfection are described in the Supplemental Information. Bacteria were grown under T1-inducing conditions in LB (0.3 M NaCl) as described (Misselwitz et al., 2011a).

siRNA Screen

Cell culture in 96- or 384-well format, reverse RNA transfection, controls, infection, staining, automated imaging, and automated image analysis were performed in HeLa CCL-2 using the InfectX pipeline as described in the Supplemental Information. RNA libraries included the Dharmacon ON-TARGETplus SMARTpool Library (18.237 genes), customized siRNA libraries (Ambion Silencer and Silencer Select; esiRNAs [Sigma]), and kinome-targeting siRNAs (see Supplemental Information; Table S1B). The pathogen-specific control siRNAs present in every screening plate were ArpC3, Cdc42, and ATP6V1A (reduced infection) and ITGAV and CFL1 (enhanced infection) (Misselwitz et al., 2011a). Cells were infected for 20 min with *S*.Tm^{SopE} harboring pM975 (T2-*gfp* reporter; MOI = 80), incubated for 3 hr and 40 min in medium with 400 μg/ml gentamicin, fixed (4% PFA, 4% sucrose), and stained with DAPI and DY-547-phalloidin. All liquid handling steps (infection, fixation, and staining) were performed with a liquid handling robot (BioTek; EL406). After high-throughput image acquisition of the 384-well screening plates using the Molecular Devices ImageXpress microscope (10X S Fluor; 1,000–3,500 cells per well), a CellProfiler-based image analysis pipeline was applied. The analysis involved shading correction to compensate for uneven microscope-based illumination and detected SCV-residing *S*.Tm through a wavelet-based small particle detector CellProfiler module. Herewith, we extracted on average 550 features for five distinct objects (bacteria, nuclei, cells, perinuclei, and voronoi cells) out of 1.8 million images and in total more than 100 million cells.

Step-Specific Assays

Assays were performed as described (Misselwitz et al., 2011a; for details, see Supplemental Information). Binding to MEF was analyzed by 6 min *S*.Tm$^{\Delta 4}$ infection (MOI = 125), washing, and automated microscopy quantification of surface-attached bacteria. Ruffling was quantified after 12 min *S*.Tm^{SopE} (pM965; MOI = 80) infection, phalloidin staining, z stack imaging, and blinded quantification of membrane ruffles. The classical gentamicin-protection assay was performed in 20 min infections (MOI = 10), subsequent incubation in gentamicin medium for the indicated times, and plating-enumeration of the remaining intracellular bacteria. For helper assays and invasion-mediated invasion, higher MOIs were applied (see Supplemental Information).

Statistics

The number of biological replicates was sufficient to perform statistics using the non-parametric Mann-Whitney U test, comparing individual data points for experimental and control samples.

Fluorescence Microcopy and Quantitative Analysis of Co-localization

Cells transfected or dye-dextran-loaded (FITC-dextran, 500 kDa; Blue-dextran, 500 kDa) were infected as indicated and exposed to osmotic shock (as indicated), fixed and stained, and imaged with a 100× objective, a spinning disc head, and a Zeiss Axiovert 200 m microscope, and marker co-localization was analyzed with Volocity (quantitation module) as detailed in the Supplemental Information.

SUPPLEMENTAL INFORMATION

Supplemental Information includes Supplemental Experimental Procedures, six figures, and one table and can be found with this article online at http://dx.doi.org/10.1016/j.chom.2015.10.015.

AUTHOR CONTRIBUTIONS

S.K. and W.D.H. designed the experiments; S.K. performed the experiments; J.F. performed EM; M.E. and P.R. analyzed screening data; M.E., P.R., and C.D. contributed to data analysis; J.F. and J.E. provided Galectin-3 constructs and supported design of experiments; C.M. provided ATG5-deficient murine fibroblasts and helped throughout discussions; and S.K. and W.D.H. wrote the manuscript.

ACKNOWLEDGMENTS

We thank F. Randow, D.W. Holden, M.E. Sellin, Hardt lab members, and the members of InfectX/TargetInfectX and ScopeM, i.e., F. Schmich, D. Andritschke, and J. Mercer (also for marker constructs), for help with the GWS and in-depth discussions. M. Sachse, J. Krijnse-Locker (Institut Pasteur Ultrapole), and A. Weiner provided invaluable help with correlative EM. The work was funded by SystemsX.ch, the Swiss Initiative in Systems Biology, RTD grants 51RT-0_126008 (InfectX) and 51RTP0_151029 (TargetInfectX), evaluated by the Swiss National Science Foundation and Swiss National Science Foundation grant 310030_153074/1 to W.D.H. Further support was received from SyBIT, the IT project of SystemsX. J.E. is a member of the LabEx consortium IBEID and is supported by the Institut Pasteur CARNOT-MIE programme and an ERC starting grant (Rupteffects, No. 261166). J.F. was supported by a Pasteur Foundation fellowship.

Received: June 26, 2015
Revised: September 19, 2015
Accepted: October 26, 2015
Published: November 11, 2015

REFERENCES

Ackermann, M., Stecher, B., Freed, N.E., Songhet, P., Hardt, W.D., and Doebeli, M. (2008). Self-destructive cooperation mediated by phenotypic noise. Nature *454*, 987–990.

Amer, A.O., and Swanson, M.S. (2005). Autophagy is an immediate macrophage response to Legionella pneumophila. Cell. Microbiol. *7*, 765–778.

Bakowski, M.A., Braun, V., and Brumell, J.H. (2008). Salmonella-containing vacuoles: directing traffic and nesting to grow. Traffic *9*, 2022–2031.

Baxt, L.A., Garza-Mayers, A.C., and Goldberg, M.B. (2013). Bacterial subversion of host innate immune pathways. Science *340*, 697–701.

Benjamin, J.L., Sumpter, R., Jr., Levine, B., and Hooper, L.V. (2013). Intestinal epithelial autophagy is essential for host defense against invasive bacteria. Cell Host Microbe *13*, 723–734.

Berón, W., Gutierrez, M.G., Rabinovitch, M., and Colombo, M.I. (2002). Coxiella burnetii localizes in a Rab7-labeled compartment with autophagic characteristics. Infect. Immun. *70*, 5816–5821.

Birmingham, C.L., Smith, A.C., Bakowski, M.A., Yoshimori, T., and Brumell, J.H. (2006). Autophagy controls Salmonella infection in response to damage to the Salmonella-containing vacuole. J. Biol. Chem. *281*, 11374–11383.

Braun, V., Wong, A., Landekic, M., Hong, W.J., Grinstein, S., and Brumell, J.H. (2010). Sorting nexin 3 (SNX3) is a component of a tubular endosomal network induced by Salmonella and involved in maturation of the Salmonella-containing vacuole. Cell. Microbiol. *12*, 1352–1367.

Brumell, J.H., Tang, P., Zaharik, M.L., and Finlay, B.B. (2002). Disruption of the Salmonella-containing vacuole leads to increased replication of Salmonella enterica serovar typhimurium in the cytosol of epithelial cells. Infect. Immun. *70*, 3264–3270.

Choy, A., Dancourt, J., Mugo, B., O'Connor, T.J., Isberg, R.R., Melia, T.J., and Roy, C.R. (2012). The Legionella effector RavZ inhibits host autophagy through irreversible Atg8 deconjugation. Science *338*, 1072–1076.

Conway, K.L., Kuballa, P., Song, J.H., Patel, K.K., Castoreno, A.B., Yilmaz, O.H., Jijon, H.B., Zhang, M., Aldrich, L.N., Villablanca, E.J., et al. (2013). Atg16l1 is required for autophagy in intestinal epithelial cells and protection of mice from Salmonella infection. Gastroenterology *145*, 1347–1357.

Diard, M., Garcia, V., Maier, L., Remus-Emsermann, M.N., Regoes, R.R., Ackermann, M., and Hardt, W.D. (2013). Stabilization of cooperative virulence by the expression of an avirulent phenotype. Nature *494*, 353–356.

Figueira, R., and Holden, D.W. (2012). Functions of the Salmonella pathogenicity island 2 (SPI-2) type III secretion system effectors. Microbiology *158*, 1147–1161.

Fontayne, A., Dang, P.M., Gougerot-Pocidalo, M.A., and El-Benna, J. (2002). Phosphorylation of p47phox sites by PKC alpha, beta II, delta, and zeta: effect on binding to p22phox and on NADPH oxidase activation. Biochemistry *41*, 7743–7750.

Franceschini, A., Meier, R., Casanova, A., Kreibich, S., Daga, N., Andritschke, D., Dilling, S., Rämö, P., Emmenlauer, M., Kaufmann, A., et al. (2014). Specific inhibition of diverse pathogens in human cells by synthetic microRNA-like oligonucleotides inferred from RNAi screens. Proc. Natl. Acad. Sci. USA *111*, 4548–4553.

Fredlund, J., and Enninga, J. (2014). Cytoplasmic access by intracellular bacterial pathogens. Trends Microbiol. *22*, 128–137.

Fujita, N., Itoh, T., Omori, H., Fukuda, M., Noda, T., and Yoshimori, T. (2008). The Atg16L complex specifies the site of LC3 lipidation for membrane biogenesis in autophagy. Mol. Biol. Cell *19*, 2092–2100.

Gutierrez, M.G., Vázquez, C.L., Munafó, D.B., Zoppino, F.C., Berón, W., Rabinovitch, M., and Colombo, M.I. (2005). Autophagy induction favours the generation and maturation of the Coxiella-replicative vacuoles. Cell. Microbiol. *7*, 981–993.

Hanada, T., Noda, N.N., Satomi, Y., Ichimura, Y., Fujioka, Y., Takao, T., Inagaki, F., and Ohsumi, Y. (2007). The Atg12-Atg5 conjugate has a novel E3-like activity for protein lipidation in autophagy. J. Biol. Chem. *282*, 37298–37302.

Hapfelmeier, S., Ehrbar, K., Stecher, B., Barthel, M., Kremer, M., and Hardt, W.D. (2004). Role of the Salmonella pathogenicity island 1 effector proteins SipA, SopB, SopE, and SopE2 in Salmonella enterica subspecies 1 serovar Typhimurium colitis in streptomycin-pretreated mice. Infect. Immun. *72*, 795–809.

Hardt, W.D., Chen, L.M., Schuebel, K.E., Bustelo, X.R., and Galán, J.E. (1998). S. typhimurium encodes an activator of Rho GTPases that induces membrane ruffling and nuclear responses in host cells. Cell *93*, 815–826.

Harrison, R.E., Brumell, J.H., Khandani, A., Bucci, C., Scott, C.C., Jiang, X., Finlay, B.B., and Grinstein, S. (2004). Salmonella impairs RILP recruitment to Rab7 during maturation of invasion vacuoles. Mol. Biol. Cell *15*, 3146–3154.

Hautefort, I., Proença, M.J., and Hinton, J.C. (2003). Single-copy green fluorescent protein gene fusions allow accurate measurement of Salmonella gene expression in vitro and during infection of mammalian cells. Appl. Environ. Microbiol. *69*, 7480–7491.

Hoffmann, C., Galle, M., Dilling, S., Käppeli, R., Müller, A.J., Songhet, P., Beyaert, R., and Hardt, W.D. (2010). In macrophages, caspase-1 activation by SopE and the type III secretion system-1 of S. typhimurium can proceed in the absence of flagellin. PLoS ONE *5*, e12477.

Hoiseth, S.K., and Stocker, B.A. (1981). Aromatic-dependent Salmonella typhimurium are non-virulent and effective as live vaccines. Nature *291*, 238–239.

Huang, J., and Brumell, J.H. (2014). Bacteria-autophagy interplay: a battle for survival. Nat. Rev. Microbiol. *12*, 101–114.

Huang, J., Canadien, V., Lam, G.Y., Steinberg, B.E., Dinauer, M.C., Magalhaes, M.A., Glogauer, M., Grinstein, S., and Brumell, J.H. (2009). Activation of antibacterial autophagy by NADPH oxidases. Proc. Natl. Acad. Sci. USA *106*, 6226–6231.

Isberg, R.R., and Van Nhieu, G.T. (1995). The mechanism of phagocytic uptake promoted by invasin-integrin interaction. Trends Cell Biol. *5*, 120–124.

Isberg, R.R., Voorhis, D.L., and Falkow, S. (1987). Identification of invasin: a protein that allows enteric bacteria to penetrate cultured mammalian cells. Cell *50*, 769–778.

Ivanov, S., and Roy, C.R. (2009). NDP52: the missing link between ubiquitinated bacteria and autophagy. Nat. Immunol. *10*, 1137–1139.

Kaiser, P., Diard, M., Stecher, B., and Hardt, W.D. (2012). The streptomycin mouse model for Salmonella diarrhea: functional analysis of the microbiota, the pathogen's virulence factors, and the host's mucosal immune response. Immunol. Rev. *245*, 56–83.

Kaniga, K., Bossio, J.C., and Galán, J.E. (1994). The Salmonella typhimurium invasion genes invF and invG encode homologues of the AraC and PulD family of proteins. Mol. Microbiol. *13*, 555–568.

Knodler, L.A., Vallance, B.A., Celli, J., Winfree, S., Hansen, B., Montero, M., and Steele-Mortimer, O. (2010). Dissemination of invasive Salmonella via bacterial-induced extrusion of mucosal epithelia. Proc. Natl. Acad. Sci. USA *107*, 17733–17738.

Knodler, L.A., Nair, V., and Steele-Mortimer, O. (2014). Quantitative assessment of cytosolic Salmonella in epithelial cells. PLoS ONE *9*, e84681.

Kuballa, P., Huett, A., Rioux, J.D., Daly, M.J., and Xavier, R.J. (2008). Impaired autophagy of an intracellular pathogen induced by a Crohn's disease associated ATG16L1 variant. PLoS ONE *3*, e3391.

Kuma, A., Hatano, M., Matsui, M., Yamamoto, A., Nakaya, H., Yoshimori, T., Ohsumi, Y., Tokuhisa, T., and Mizushima, N. (2004). The role of autophagy during the early neonatal starvation period. Nature *432*, 1032–1036.

Levine, B., Mizushima, N., and Virgin, H.W. (2011). Autophagy in immunity and inflammation. Nature *469*, 323–335.

Luo, W., and Brouwer, C. (2013). Pathview: an R/Bioconductor package for pathway-based data integration and visualization. Bioinformatics *29*, 1830–1831.

Malik-Kale, P., Winfree, S., and Steele-Mortimer, O. (2012). The bimodal lifestyle of intracellular Salmonella in epithelial cells: replication in the cytosol obscures defects in vacuolar replication. PLoS ONE *7*, e38732.

Mallo, G.V., Espina, M., Smith, A.C., Terebiznik, M.R., Alemán, A., Finlay, B.B., Rameh, L.E., Grinstein, S., and Brumell, J.H. (2008). SopB promotes phosphatidylinositol 3-phosphate formation on Salmonella vacuoles by recruiting Rab5 and Vps34. J. Cell Biol. *182*, 741–752.

Marchiando, A.M., Ramanan, D., Ding, Y., Gomez, L.E., Hubbard-Lucey, V.M., Maurer, K., Wang, C., Ziel, J.W., van Rooijen, N., Nuñez, G., et al. (2013). A deficiency in the autophagy gene Atg16L1 enhances resistance to enteric bacterial infection. Cell Host Microbe *14*, 216–224.

Mirold, S., Ehrbar, K., Weissmüller, A., Prager, R., Tschäpe, H., Rüssmann, H., and Hardt, W.D. (2001). Salmonella host cell invasion emerged by acquisition of a mosaic of separate genetic elements, including Salmonella pathogenicity island 1 (SPI1), SPI5, and sopE2. J. Bacteriol. *183*, 2348–2358.

Misselwitz, B., Dilling, S., Vonaesch, P., Sacher, R., Snijder, B., Schlumberger, M., Rout, S., Stark, M., von Mering, C., Pelkmans, L., and Hardt, W.D. (2011a). RNAi screen of Salmonella invasion shows role of COPI in membrane targeting of cholesterol and Cdc42. Mol. Syst. Biol. *7*, 474.

Misselwitz, B., Kreibich, S.K., Rout, S., Stecher, B., Periaswamy, B., and Hardt, W.D. (2011b). Salmonella enterica serovar Typhimurium binds to HeLa cells via Fim-mediated reversible adhesion and irreversible type three secretion system 1-mediated docking. Infect. Immun. *79*, 330–341.

Mizushima, N., Yamamoto, A., Hatano, M., Kobayashi, Y., Kabeya, Y., Suzuki, K., Tokuhisa, T., Ohsumi, Y., and Yoshimori, T. (2001). Dissection of autophagosome formation using Apg5-deficient mouse embryonic stem cells. J. Cell Biol. *152*, 657–668.

Mizushima, N., Kuma, A., Kobayashi, Y., Yamamoto, A., Matsubae, M., Takao, T., Natsume, T., Ohsumi, Y., and Yoshimori, T. (2003). Mouse Apg16L, a novel WD-repeat protein, targets to the autophagic isolation membrane with the Apg12-Apg5 conjugate. J. Cell Sci. *116*, 1679–1688.

Müller, A.J., Hoffmann, C., Galle, M., Van Den Broeke, A., Heikenwalder, M., Falter, L., Misselwitz, B., Kremer, M., Beyaert, R., and Hardt, W.D. (2009). The S. Typhimurium effector SopE induces caspase-1 activation in stromal cells to initiate gut inflammation. Cell Host Microbe *6*, 125–136.

Nakagawa, I., Amano, A., Mizushima, N., Yamamoto, A., Yamaguchi, H., Kamimoto, T., Nara, A., Funao, J., Nakata, M., Tsuda, K., et al. (2004). Autophagy defends cells against invading group A Streptococcus. Science *306*, 1037–1040.

Ogawa, M., Yoshimori, T., Suzuki, T., Sagara, H., Mizushima, N., and Sasakawa, C. (2005). Escape of intracellular Shigella from autophagy. Science *307*, 727–731.

Rathman, M., Sjaastad, M.D., and Falkow, S. (1996). Acidification of phagosomes containing Salmonella typhimurium in murine macrophages. Infect. Immun. *64*, 2765–2773.

Romano, P.S., Gutierrez, M.G., Berón, W., Rabinovitch, M., and Colombo, M.I. (2007). The autophagic pathway is actively modulated by phase II Coxiella burnetii to efficiently replicate in the host cell. Cell. Microbiol. *9*, 891–909.

Saini, S., Ellermeier, J.R., Slauch, J.M., and Rao, C.V. (2010). Correction: The role of coupled positive feedback in the expression of the SPI1 type three secretion system in Salmonella. PLoS Pathog. *6*, http://dx.doi.org/10.1371/annotation/df7e26bc-4c62-43b4-865f-a39274d98ab3.

Schlumberger, M.C., and Hardt, W.D. (2006). Salmonella type III secretion effectors: pulling the host cell's strings. Curr. Opin. Microbiol. *9*, 46–54.

Schlumberger, M.C., Müller, A.J., Ehrbar, K., Winnen, B., Duss, I., Stecher, B., and Hardt, W.D. (2005). Real-time imaging of type III secretion: Salmonella SipA injection into host cells. Proc. Natl. Acad. Sci. USA *102*, 12548–12553.

Schlumberger, M.C., Käppeli, R., Wetter, M., Müller, A.J., Misselwitz, B., Dilling, S., Kremer, M., and Hardt, W.D. (2007). Two newly identified SipA domains (F1, F2) steer effector protein localization and contribute to Salmonella host cell manipulation. Mol. Microbiol. *65*, 741–760.

Shahnazari, S., Yen, W.L., Birmingham, C.L., Shiu, J., Namolovan, A., Zheng, Y.T., Nakayama, K., Klionsky, D.J., and Brumell, J.H. (2010). A diacylglycerol-dependent signaling pathway contributes to regulation of antibacterial autophagy. Cell Host Microbe *8*, 137–146.

Shahnazari, S., Namolovan, A., Klionsky, D.J., and Brumell, J.H. (2011). A role for diacylglycerol in antibacterial autophagy. Autophagy *7*, 331–333.

Smith, A.C., Cirulis, J.T., Casanova, J.E., Scidmore, M.A., and Brumell, J.H. (2005). Interaction of the Salmonella-containing vacuole with the endocytic recycling system. J. Biol. Chem. *280*, 24634–24641.

Smith, A.C., Heo, W.D., Braun, V., Jiang, X., Macrae, C., Casanova, J.E., Scidmore, M.A., Grinstein, S., Meyer, T., and Brumell, J.H. (2007). A network of Rab GTPases controls phagosome maturation and is modulated by Salmonella enterica serovar Typhimurium. J. Cell Biol. *176*, 263–268.

Starr, T., Child, R., Wehrly, T.D., Hansen, B., Hwang, S., López-Otin, C., Virgin, H.W., and Celli, J. (2012). Selective subversion of autophagy complexes facilitates completion of the Brucella intracellular cycle. Cell Host Microbe *11*, 33–45.

Steele-Mortimer, O., Brumell, J.H., Knodler, L.A., Méresse, S., Lopez, A., and Finlay, B.B. (2002). The invasion-associated type III secretion system of Salmonella enterica serovar Typhimurium is necessary for intracellular proliferation and vacuole biogenesis in epithelial cells. Cell. Microbiol. *4*, 43–54.

Sturm, A., Heinemann, M., Arnoldini, M., Benecke, A., Ackermann, M., Benz, M., Dormann, J., and Hardt, W.D. (2011). The cost of virulence: retarded growth of Salmonella Typhimurium cells expressing type III secretion system 1. PLoS Pathog. *7*, e1002143.

Tattoli, I., Sorbara, M.T., Vuckovic, D., Ling, A., Soares, F., Carneiro, L.A., Yang, C., Emili, A., Philpott, D.J., and Girardin, S.E. (2012). Amino acid starvation induced by invasive bacterial pathogens triggers an innate host defense program. Cell Host Microbe *11*, 563–575.

Thurston, T.L., Ryzhakov, G., Bloor, S., von Muhlinen, N., and Randow, F. (2009). The TBK1 adaptor and autophagy receptor NDP52 restricts the proliferation of ubiquitin-coated bacteria. Nat. Immunol. *10*, 1215–1221.

Thurston, T.L., Wandel, M.P., von Muhlinen, N., Foeglein, A., and Randow, F. (2012). Galectin 8 targets damaged vesicles for autophagy to defend cells against bacterial invasion. Nature *482*, 414–418.

Watson, R.O., Manzanillo, P.S., and Cox, J.S. (2012). Extracellular M. tuberculosis DNA targets bacteria for autophagy by activating the host DNA-sensing pathway. Cell *150*, 803–815.

Wild, P., Farhan, H., McEwan, D.G., Wagner, S., Rogov, V.V., Brady, N.R., Richter, B., Korac, J., Waidmann, O., Choudhary, C., et al. (2011). Phosphorylation of the autophagy receptor optineurin restricts Salmonella growth. Science *333*, 228–233.

Winnen, B., Schlumberger, M.C., Sturm, A., Schüpbach, K., Siebenmann, S., Jenny, P., and Hardt, W.D. (2008). Hierarchical effector protein transport by the Salmonella Typhimurium SPI-1 type III secretion system. PLoS ONE *3*, e2178.

Yoshikawa, Y., Ogawa, M., Hain, T., Yoshida, M., Fukumatsu, M., Kim, M., Mimuro, H., Nakagawa, I., Yanagawa, T., Ishii, T., et al. (2009). Listeria monocytogenes ActA-mediated escape from autophagic recognition. Nat. Cell Biol. *11*, 1233–1240.

Yu, X.J., McGourty, K., Liu, M., Unsworth, K.E., and Holden, D.W. (2010). pH sensing by intracellular Salmonella induces effector translocation. Science *328*, 1040–1043.

Yu, H.B., Croxen, M.A., Marchiando, A.M., Ferreira, R.B., Cadwell, K., Foster, L.J., and Finlay, B.B. (2014). Autophagy facilitates Salmonella replication in HeLa cells. MBio *5*, e00865–e14.

Zheng, Y.T., Shahnazari, S., Brech, A., Lamark, T., Johansen, T., and Brumell, J.H. (2009). The adaptor protein p62/SQSTM1 targets invading bacteria to the autophagy pathway. J. Immunol. *183*, 5909–5916.